Evaluating the Surface Finish of A356-T6 Cast Parts from Additively Manufactured Sand Molds

Caitlyn Rodomsky[1,2] and Brett Conner[1]

[1]Youngstown State University
[2]Applied Systems and Technology Transfer, LLC

Abstract:

Binder jetting of sand allows for the design and rapid fabrication of complex molds and cores. The surface finish of the printed molds and cores can be transferred to the cast part. A benchmark casting was designed to compare the surface roughness and surface features of several angles on the cast part. The benchmark casting contained surfaces with angles from 5° to 30° at 5° intervals. Benchmark castings from coated and uncoated mold surfaces were evaluated. Angles from 5° to 20° produced a prominent stair step feature. A Keyence microscope was used to measure the arithmetic mean roughness (Ra) and root mean square surface roughness (Rq) of the part surfaces. These measurements are compared to a more conventional contact profilometer. The suitability of Ra and Rq for characterizing stair step features will be discussed.

Keywords: surface roughness, stair step features, binder jetting, sand printing, metal castings

1. Introduction

In 2016, the global production of metal castings was 104.4 million metric tons [1]. In the United States alone, there are nearly 2,000 metal casting facilities in the country [1]. Although there are many processes for metal casting, sand casting remains one of the most widely used casting processes [2]. Over 70% of all metal castings are produced via sand casting, and the sand casting industry supplies parts to market sectors such as energy, aerospace and automotive [3].

The conventional approach to sand casting tooling is to machine hard tooling such as patterns and core boxes. In many cases, hard tooling can be expensive and have long lead times. This is especially true if the casting is geometrically complex. As shown in [4], 3D sand printing can produce molds and cores more cost effectively at greater levels of complexity and/or at low production quantities. 3D sand printing has multiple benefits including on-demand production of molds and cores without the need for hard tooling, core consolidation (thereby eliminating or mitigating core shift, flash, and core assembly damage), affordable low quantity production, and simplifying the fabrication of complex gating designs. 3D sand printing of cores can be combined with conventional hard molds or 3D printed hard molds for greater cost effectiveness

when exterior mold lines are relatively simple and production quantities are high [5]. Finally, 3D sand printed molds and cores can be embedded with multi-modality wireless sensor devices to provide data for quality management and solidification model validation [6].

A common method for 3D printing of sand molds is binder jetting. The ISO standard for additive manufacturing (AM) terminology defines binder jetting as an "additive manufacturing process in which a liquid bonding agent is selectively deposited to join powder materials." [7]. In binder jetting for sand printing, a layer of sand is evenly spread by a recoater over the build volume. Next, the inkjet head sprays a foundry-ready binder (such as furan or phenolic) anywhere a part intersects the layer. The build box has a false floor that lowers one layer thickness, t, in the negative z-direction. This process is repeated until the build is complete. The build box can be removed from the 3D printer to facilitate depowdering operations.

Like many additive manufacturing processes, layerwise fabrication can produce stair step features in the printed mold or core. The steps in the mold can be transferred to the casting. The stair step features in the casting can change aesthetic appearances. They can also require post-processing machining or grinding for removal. Finally, these steps could be stress concentrators that could lead to crack initiation especially in the presence of cyclic loading resulting in fatigue.

One can describe stair step features by defining a "print angle." As shown in Figure 1 on the left, the z-axis is the build direction. The print angle is the angle between the x-y plane in a given direction (or vector) as shown on the right in Figure 2. Parallel to the x-y plane is $\theta=0^{\circ}$ while perpendicular to the x-y plane (and parallel to the z-axis) is $\theta=90^{\circ}$. In theory, the layerwise printing process should create stair step features at any angle between 0° and 90° because layers have a finite thickness, t. As will be seen here, those steps may become less visible at certain angles because of the background surface topology due to the sand itself.
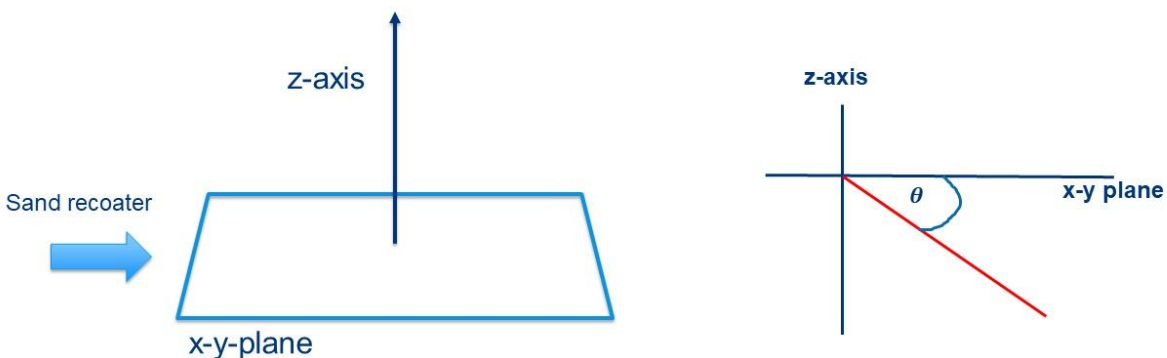

Figure 1: A schematic of the orientation of the x-y plane and the build direction are shown at the left. On the right, the print angle is shown based on the angle of the surface from the x-y plane.

The objective of the project is to determine if the surface roughness influences the mechanical properties of a casting using additively manufactured sand printed molds. The following research questions will be addressed in this project:

1.) What are the characteristics of casting surface features that are associated with the print angle?

2.) Can the surface texture of stair step features be quantified using arithmetic mean roughness (Ra) and the root mean square height (Rq)? Are those measures useful for these and other sand printing features? Can Ra and Rq be expressed as a function of print angle?

3.) Can a refractory coating such as Dura Kote eliminate stair step features?

4.) Are the differences in the surface features between upward facing casting surfaces and downward facing casting surfaces?

2. Methodology

2.1 Benchmark casting design

The main purpose of designing a benchmark casting is to use a single casting to determine the size and space of stair step features and to measure the surface roughness of the part surfaces cast at different print angle orientations in the mold. The benchmark casting required multiple surfaces that are at an angle to the build direction. The design for the benchmark casting involved a round four-inch casting that contains six different print orientation angles. These angles consist of 5°, 10°, 15°, 20°, 25°, and 30°. The benchmark is shown in Figure 2.
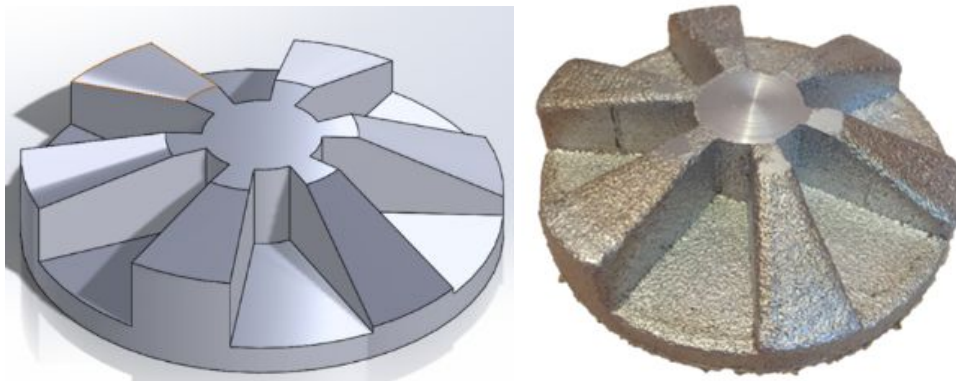

Figure 2: Benchmark casting (left) isometric CAD and (right) the casting itself

The mold was designed to include two benchmark castings per mold: one upward facing and one downward facing. This permitted observation of differences in surface features resulting from upward or downward mold surfaces. Figure 3 shows the gating system for this pair of

castings. The upward facing casting is to the left in Figure 3 and the downward facing to the right. This gating system consisted of one pour cup, one sprue, one sprue basin, two gates to feed the casting, and two tapered feeders/vents.
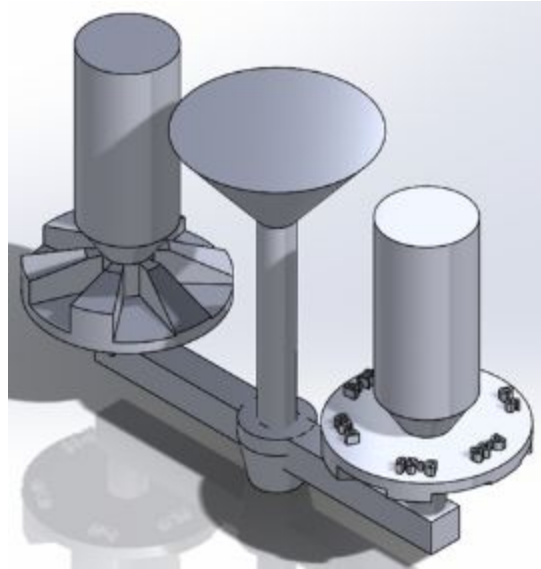

Figure 3: Benchmark part with gating system

The gating geometry shown in Figure 3 prevents a flat parting line. This is not a challenge for 3D sand printing so a staggered parting line that ran at the bottom of the two parts can be seen in Figure 4. This mold contained lifting holds on both sides for the cope and drag. These are inserted to help lift the mold for cleaning and assembly. The pegs on the cope are designed to assist with assembling the cope and drag. The pegs are tapered to prevent rubbing sand-on-sand during insertion of the pegs into the corresponding holes which could distribute debris into the cavity. Assembly instructions were extruded into mold faces and the casting weight of 5.81 lbs was extruded into the top of the cope to ensure that metal was not wasted.
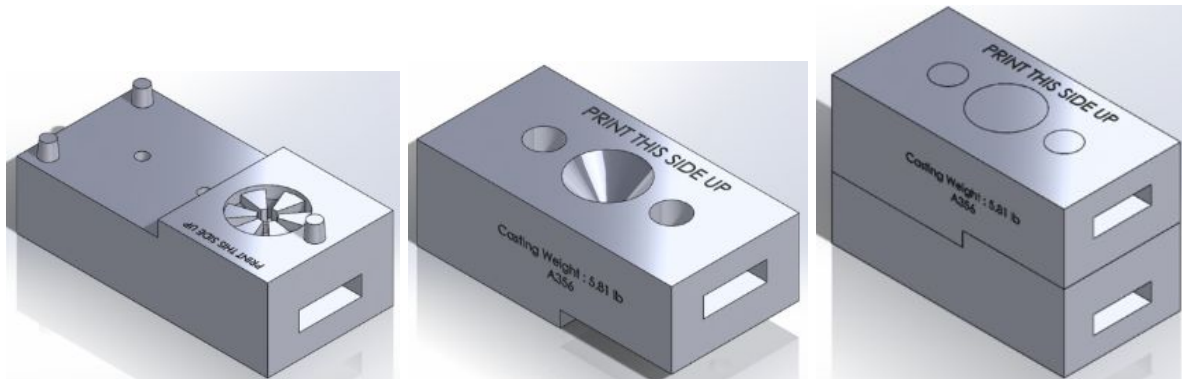

Figure 4: Mold for benchmark casting

Two molds sets were fabricated. The mold design was the same for both molds, but a coating would be applied to the surfaces of one of the mold sets to determine if it improved the surface finish of the cast A356 part. The coating on the sand mold may increase the smoothness of the surface finish of the casting and therefore decrease the post-processing on the cast part.

2.2 Flat bar design

Flat bars were designed for three point bend fatigue testing. The dimensions of the flat bar are 101.6 x 50.8 x 6.35 mm (4 x 2 x 0.25 inches). The flat bar was used to maximize the surface area containing stair step features. This also made a useful specimen to study surface features. Fatigue testing results are not included in this paper. A gating system (see Figure 5) was developed to contain multiple flat tensile bars and flat bar fatigue specimens of the same print angle. Four mold sets were fabricated for four print angles: 0°, 5°, 15°, 30°. Several of the fatigue specimens were examined using contact profilometry and comparator plate. 5 and 15° print angle flat bars (both downward facing and upward facing surfaces) are shown in Figure 6. It can be seen that the stairs are more visible on the upward facing surfaces than the downward facing surfaces.
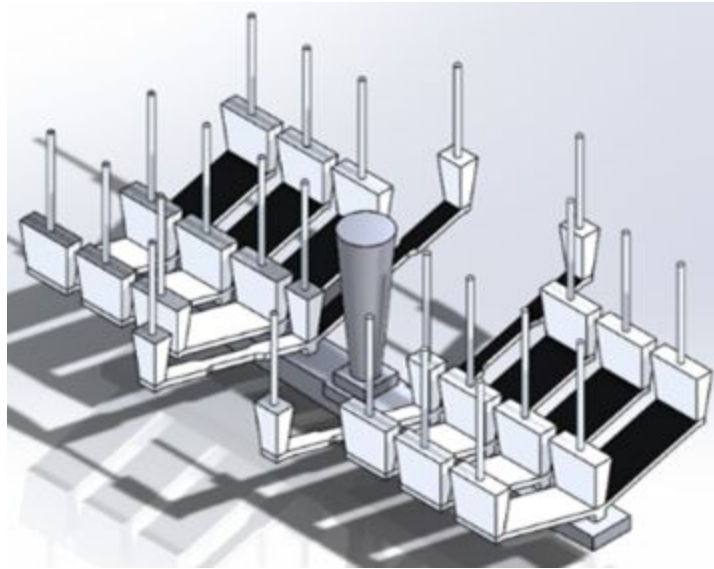

Figure 5: The gating system used for the 15° flat bar specimen casting.
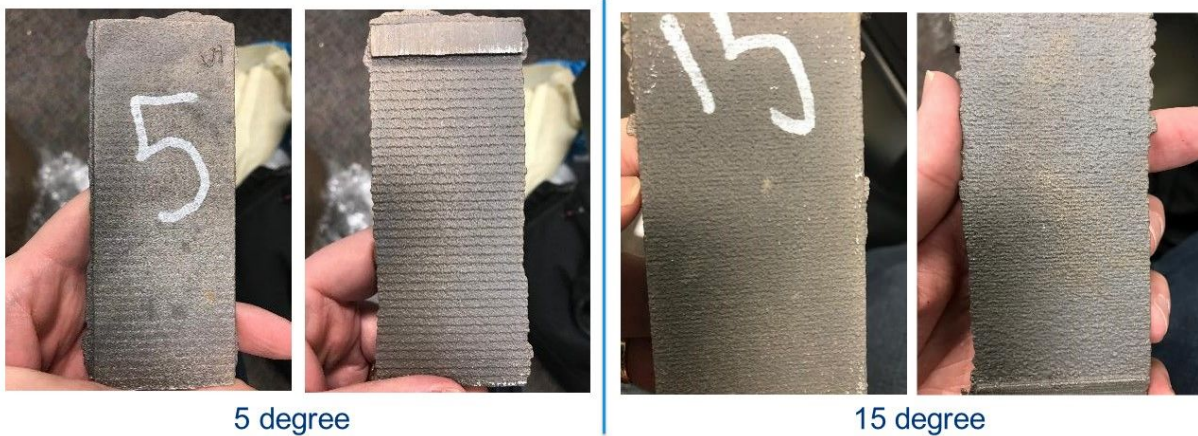
Figure 6: (Far left) 5° flat bar downward facing surface, (Left) 5° flat bar upward facing surface. (Right) 15° flat bar downward facing surface and (Far right) 15° flat bar upward facing surface

2.3 Printing

The molds for the castings were produced on YSU's ExOne S-Max 3D sand printer shown in Figure 7. This is a production-type printer that is used to produce sand molds and cores for the metal casting industry. The printer, including one job box is 6900 x 3520 x 2860 (L x W x H) mm (271 x 138.6 x 112.6 inches) and weighs 6,500 kg (14,330 pounds). The build volume is 1800 x 1000 x 700 (L x W x H) mm (70.9 x 39.4 x 27.6 inch). The build speed of the S-Max is 60,000 to 85,000 cm^3/h (2.12 to 3.00 ft^3/h). The binder system used by the printer was a furan resin which is a furfuryl alcohol. Furan is a foundry resin for green sand. The activator was a toluene sulfonic acid (TSA) and is mixed with the sand just prior to recoating [8]. The mixer is attached to the printer. The printer's recoater spreads a layer of sand that is 0.28 mm thick on the x-y plane of the build box.

Figure 7: YSU's ExOne S-Max 3D sand printer

The sand used was IC-80 Oklahoma, which has a grain fineness number (GFN) of 83 which corresponds to an average particle size between 150 to 170 μm. The grain fineness number is the average size of a granular material [9]. The higher the GFN the finer the sand and the smoother the surface of the cast part. The furan binder used was 371381 Enviroset 3D Jet Resin from HA International.

Two benchmark mold sets were printed. One of the set of benchmark molds was left uncoated. The other was coated with a refractory coating. The coating used was Dura Kote 4482 from HA International LLC. It is light blue and premixed. Dura Kote is a water-based material coating with a typical density of 19.80 lbs/gal and a Zircon refractory system [10]. The coating was applied manually using a generic paint brush and placed on the print angle surface of the benchmark casting.

The benchmark castings were cast in alloy A356 at the YSU foundry. No post-casting heat treatment was conducted on the benchmark castings. The flat bars were cast at Lite Metals Company in Ravenna, Ohio. The A356 flat bars were given a T6 temper post-process heat treatment.

2.4 Measurement

The surfaces of the benchmark castings were evaluated using a Keyence Microscope VK-X200 series non-contact 3D laser scanning confocal microscope. The Keyence uses two software packages for scan planning and compiling data: VK-Viewer and VK-Analyzer. The VK Viewer was used to select the region and direction of scanning. After scanning, the multiple line surface roughness tool in VK Analyzer was used to measure the surface finish of a cast part.

A KLA-Tencor D-100 profilometer was used for measurements of the flat bars. The Tencor profilometer is a contact sensor used to measure the roughness of a part. This is unlike the Keyence which is a non-contact system. For both the Keyence and Tencor devices, a measurement length of 12.7 mm was used. The surface finish of the flat bars were also evaluated against a C-9 cast microfinish comparator plate as shown in Figure 8. This allows for visual and tactile evaluation of the surface and provide a surface roughness in Imperial units. The comparator plate is a subjective method of measurement.

Figure 8: A cast microfinish comparator plate used to evaluate surface finish of the flat bar

3. Results and discussion

3.1 Benchmark casting

The measurements of R_a and R_q were taken on all six angles on each of the benchmark castings (Up/Bare Mold, Down/Bare Mold, Up/Coated Mold, Down/Coated Mold) using the Keyence Microscope multiple surface roughness line tool. The scans were in the center of each of the print orientation angles and taken down the steps in a 12.7 mm length. Two scans were taken per print orientation angle and then averaged to formulate the Ra and Rq values.
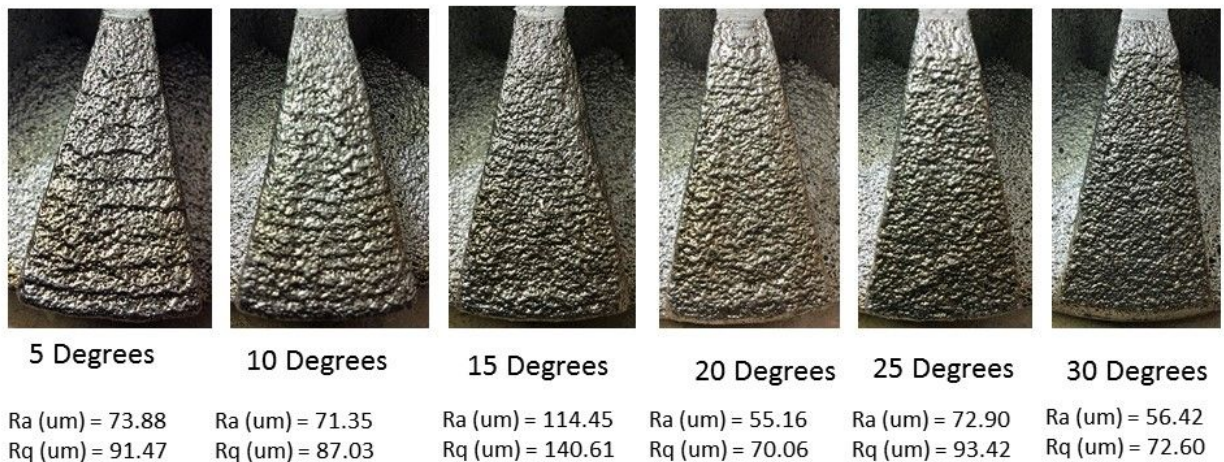

5 Degrees	10 Degrees	15 Degrees	20 Degrees	25 Degrees	30 Degrees
Ra (um) = 73.88	Ra (um) = 71.35	Ra (um) = 114.45	Ra (um) = 55.16	Ra (um) = 72.90	Ra (um) = 56.42
Rq (um) = 91.47	Rq (um) = 87.03	Rq (um) = 140.61	Rq (um) = 70.06	Rq (um) = 93.42	Rq (um) = 72.60

Figure 9: Up/Bare Mold Benchmark Casting

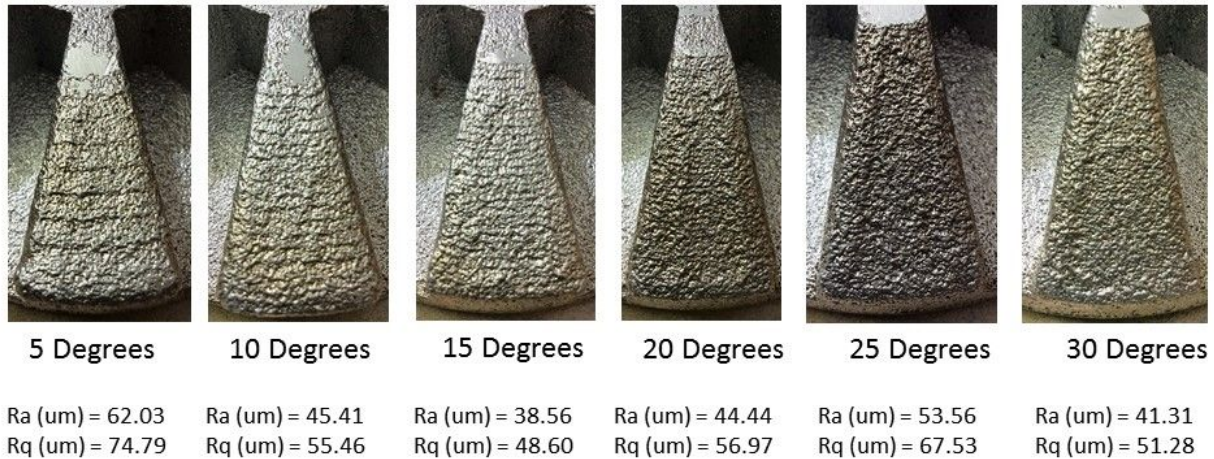| 5 Degrees	10 Degrees	15 Degrees	20 Degrees	25 Degrees	30 Degrees
Ra (um) = 62.03	Ra (um) = 45.41	Ra (um) = 38.56	Ra (um) = 44.44	Ra (um) = 53.56	Ra (um) = 41.31
Rq (um) = 74.79	Rq (um) = 55.46	Rq (um) = 48.60	Rq (um) = 56.97	Rq (um) = 67.53	Rq (um) = 51.28

Figure 10: Down/Bare Mold Benchmark Casting

In both Figure 9 and Figure 10, the stair steps are more visually prominent at angles less than or equal to 15°. By 25° or 30°, the stair steps cannot be distinguished from the background surface geometry from the sand itself. Besides stair steps, other surface defects can be seen. For example, there are depressed defects on the bottom left hand corner of 5° and 20° angle surfaces from the Up/Bare Mold benchmark casting. the print orientation angles. These can be seen in the bottom left hand corner of the 15° and 20° angles. There is also an elevated defect at the bottom middle of the 25° angle of the Up/Bare Mold benchmark casting. These could be caused by the cleanout of the molds, the packaging, or during transportation. Line-type indents can be seen on the 20°, 25° and 30° angles from the Down/Bare Mold benchmark castings. These can be caused by heavy brush strokes during sand clean out.
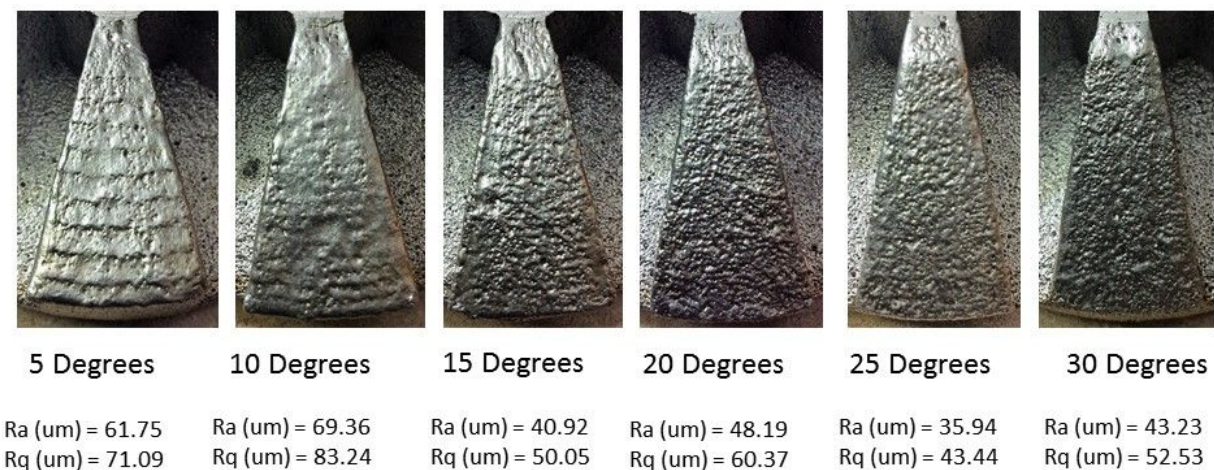

5 Degrees	10 Degrees	15 Degrees	20 Degrees	25 Degrees	30 Degrees
Ra (um) = 61.75	Ra (um) = 69.36	Ra (um) = 40.92	Ra (um) = 48.19	Ra (um) = 35.94	Ra (um) = 43.23
Rq (um) = 71.09	Rq (um) = 83.24	Rq (um) = 50.05	Rq (um) = 60.37	Rq (um) = 43.44	Rq (um) = 52.53

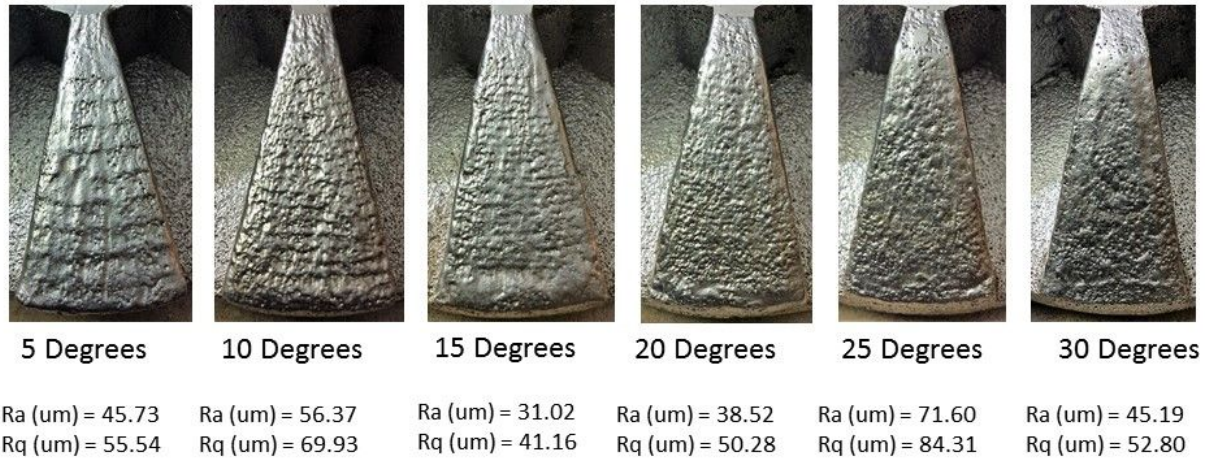**Figure 11:** Up/Coated Mold Results

Figure 12: Down/Coated Mold Results

Figures 11 and 12 show the surfaces of the castings from the coated molds. Stair step features can still be seen with the naked eye for the shallow print angles even up to 20° in Figure 12. It is apparent that the Dura Kote coating does not remove the step features. The heavy application of the coating by brush stroke for the shallow angles changes the surface texture with additional rises and depressions. The coating was also not evenly distributed throughout the entire angled surface. Keyence scans were only taken from the center of the part, so the edges were not included in the measurements.

Closer examination of the measurements for the bare mold benchmark castings show that the Ra and Rq are higher on the upward facing surfaces than the downward surfaces. As shown for the bare mold castings in Figures 13 and 14, this difference between upward and downward surfaces is consistent regardless of print angle. It is possible this has to do with the orientation of the molds during printing. As shown in Figure 4, the downward facing casting mold faced upward. Unbound sand would sit on top of the mold, which would compress the stair steps. This loose sand could also abraid the stair step features during removal. The surface roughness on the downward facing surface may also be affected by gravitational effects during the casting pour.

Ra and Rq for the castings made with coated molds can be shown in Figures 15 and 16. For the coated molds, this higher Ra and Rq on upward facing surfaces holds true for only 5° to 20° print angle surfaces. The 25° and 30° surfaces show the opposite with higher Ra and Rq for the bottom surfaces.
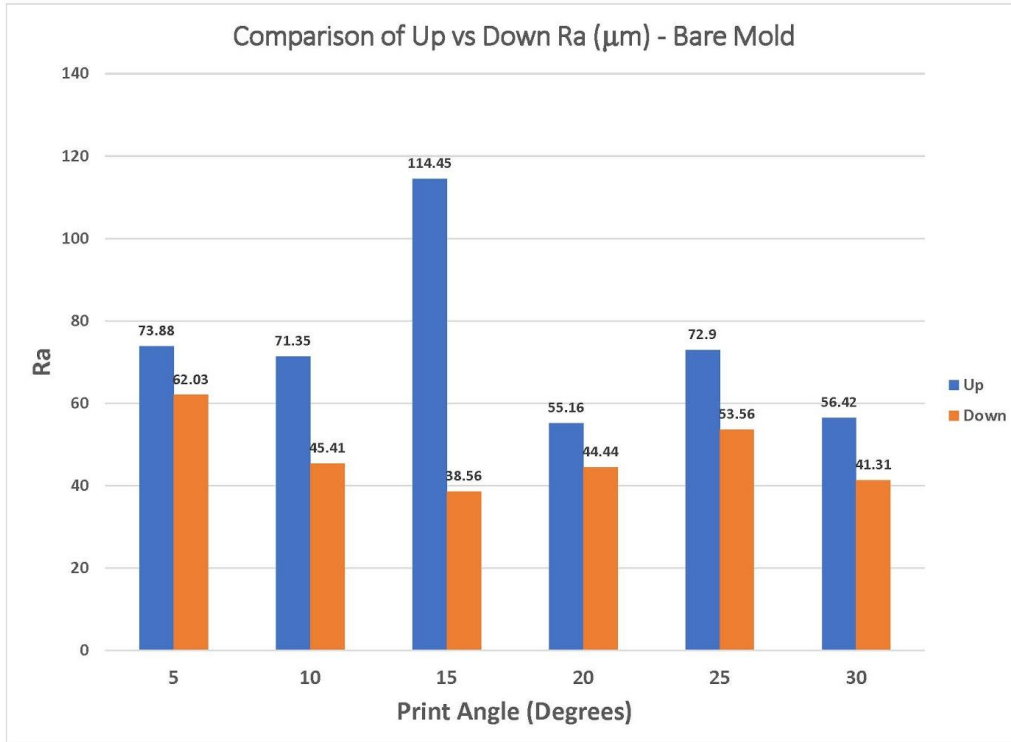
Figure 13: Ra for upward and downward facing surfaces for the benchmark casting with the bare mold.
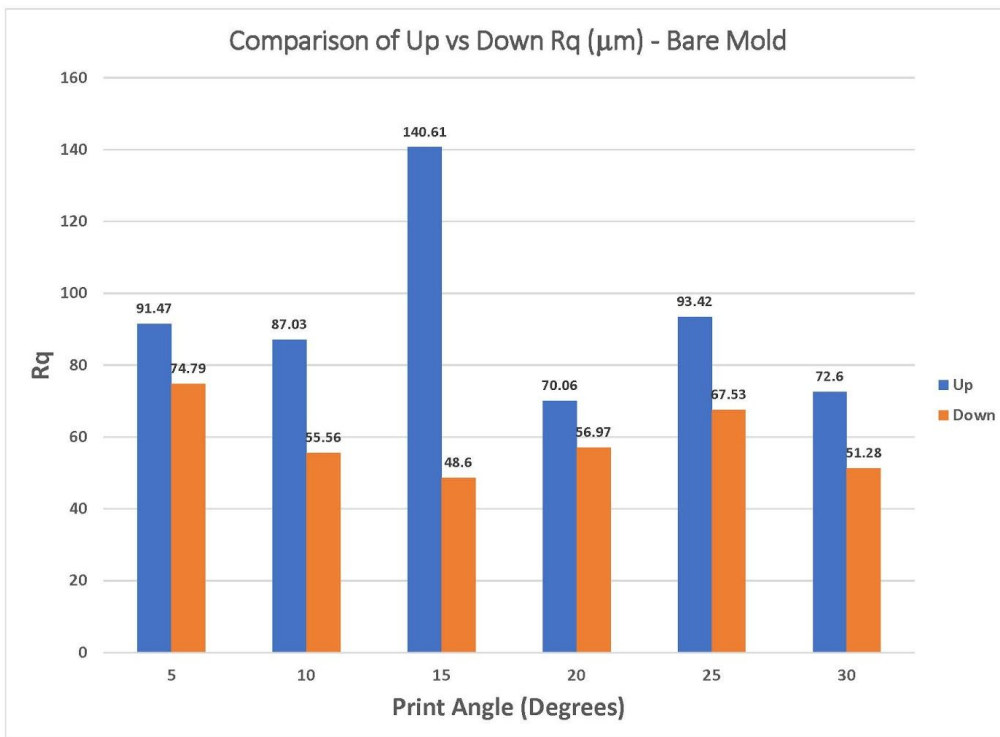

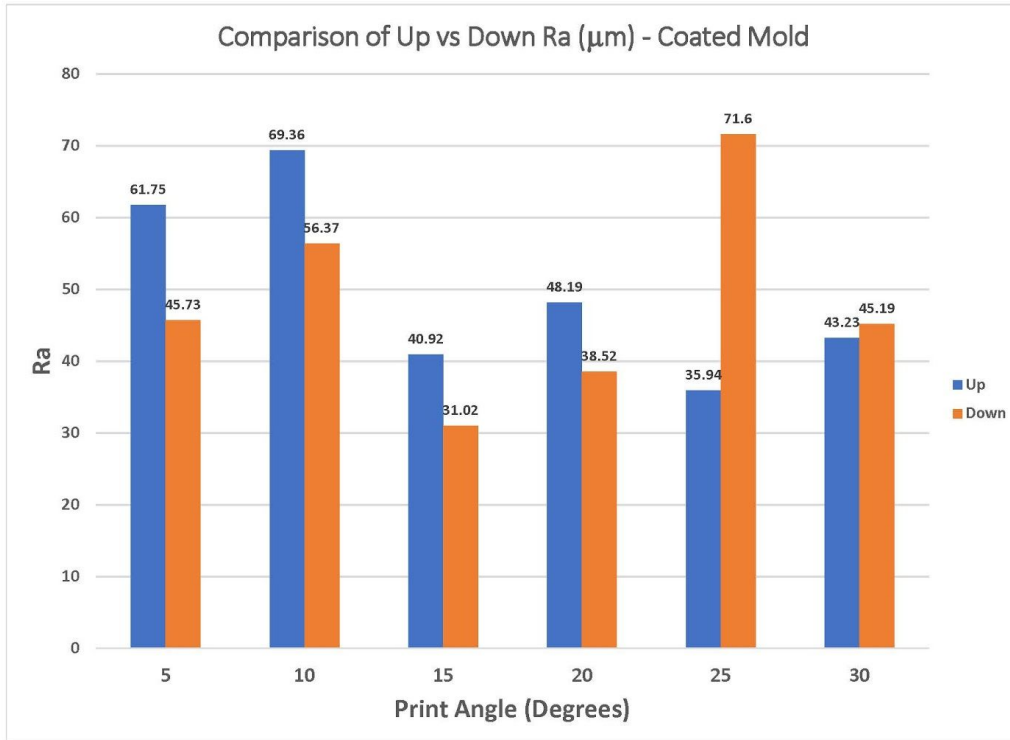**Figure 14:** Rq for upward and downward facing surfaces for the benchmark casting with the bare mold.

Figure 15: Ra for upward and downward facing surfaces for the benchmark casting with the coated mold
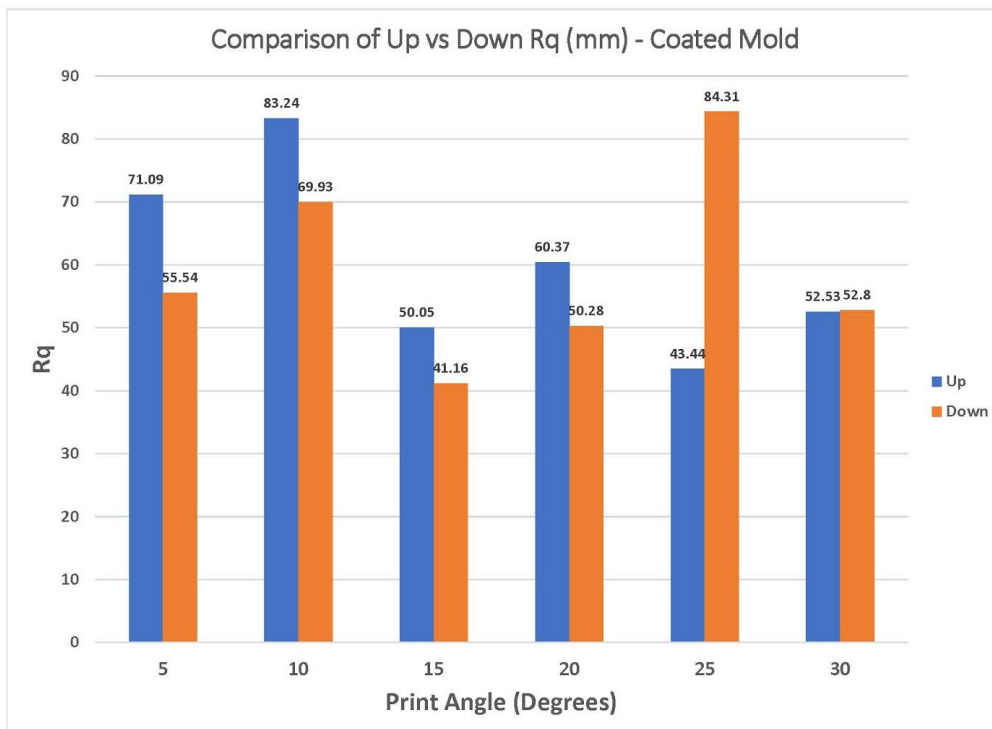

Figure 16: Rq for upward and downward facing surfaces for the benchmark casting with the coated mold.

3.2 Flat bars

The Tencor contact profilometer measurements include 0° surfaces which would show a surface without any steps in it and only a sand surface texture. As shown in Figures 17 and 18, the Ra and Rq values of the top and bottom surfaces for the 0° and 30° print angles are very close. However, the 5° and 15° print angle surfaces show the same difference between the upward surface Ra and Rq values versus the bottom ones.
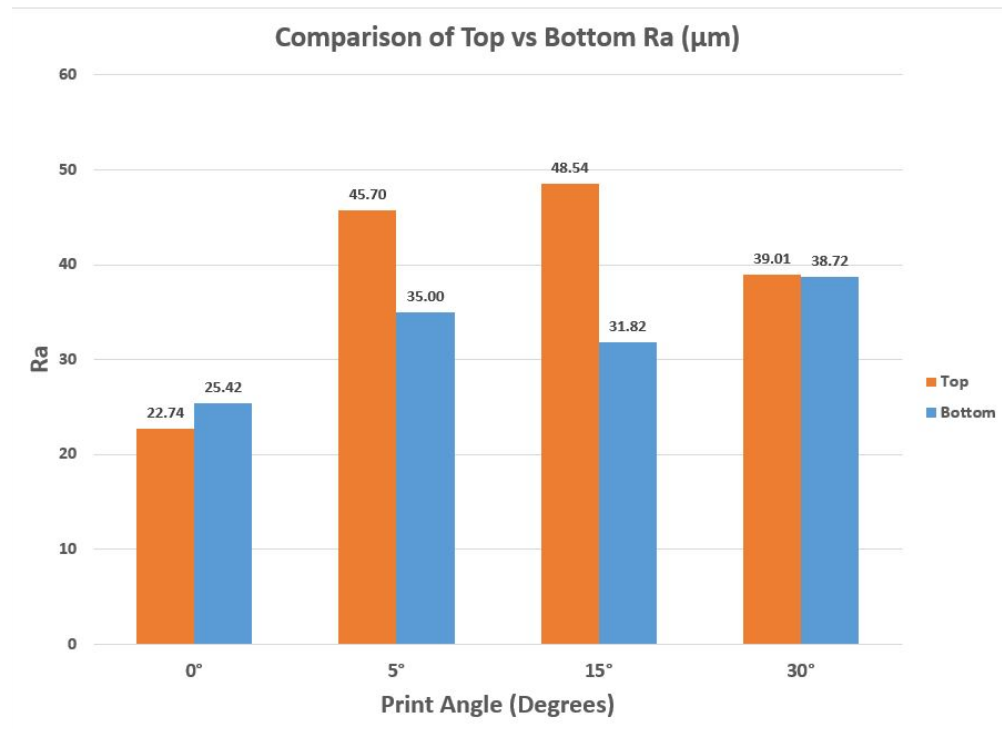

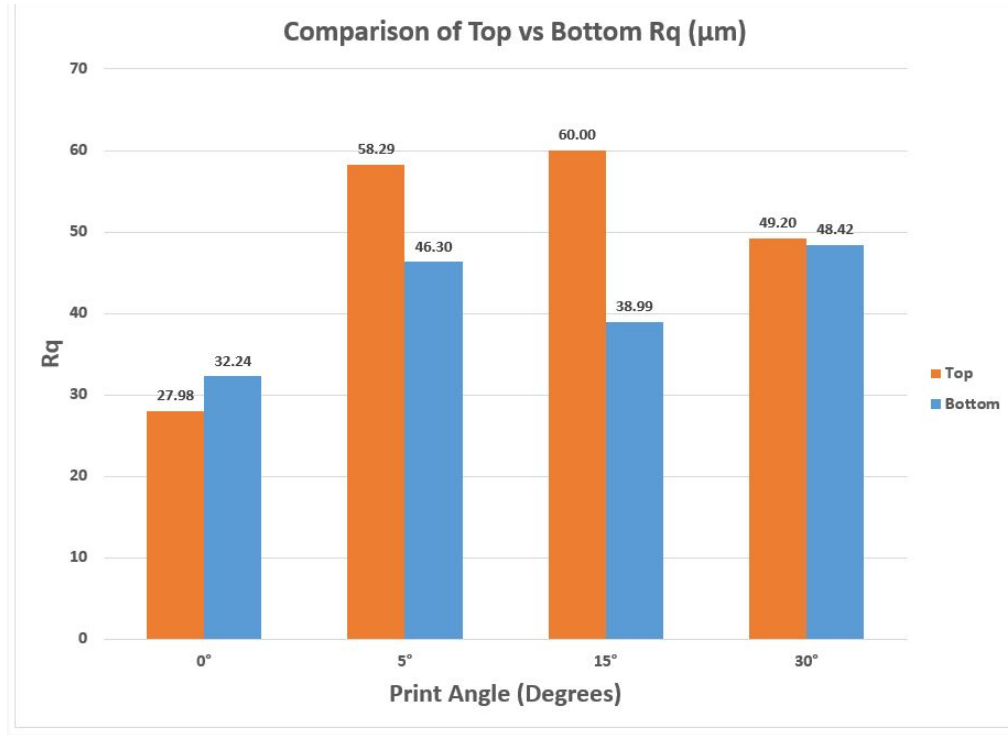**Figure 17:** Ra for upward and downward facing surfaces for the flat bar castings

Figure 18: Ra for upward and downward facing surfaces for the flat bar castings

The comparator plate was then used to evaluate the surface roughness of the flat bar specimens. Both visual inspection and touch was used. The 0° plate was evaluated to be most similar to the 420 RMS standard on the comparator plate. 420 RMS would be considered at the high end of the RMS expected for permanent mold castings (200-420) and in the middle of the range of normal non-ferrous green sand (300-560). Next, the 5° and 15° plates were evaluated to be most similar to the 720 RMS standard on the comparator plate. 560 RMS would be on the highest end of the range for normal non-ferrous green sand (300-560) and at the lowest end of the normal ferrous green sand (560-900). Finally, 30° the plate was evaluated to be most similar to the 560 RMS standard on the comparator plate. 720 RMS would be in the middle of the range for normal ferrous green sand.

3.3 Analysis of idealized surfaces

As observed in the benchmark castings, the stair steps are more visually prominent at angles less than or equal to 15°. At greater angles the steps become less visible at greater angles, and the surface of the casting appears more like the surface expected from green sand. One way to examine this is to calculate Ra and Rq for an idealized set of stair steps for surfaces at various print angles. This would then be compared to Ra and Rq calculated for a idealized sand topology: a series of close packed spheres.

We will start with the stair steps. As a reminder, the arithmetic mean roughness (Ra) indicates the average of the absolute value of height along the reference length (in our case, 12.7 mm). We will calculate in 20 steps along the reference length.

$$Ra = \frac{1}{l_r} \int_0^{l_r} |Z_n|\, dx \quad (1)$$

$$Ra = \frac{1}{n} * sum(abs\,(Z_i - Z_{mean})) \quad (2)$$

$$Z_i = total\ height$$
$$Z_{mean} = average\ height$$
$$N = 20$$

Root mean square height (Rq) – indicates the root mean square along the reference length

$$Rq = \sqrt{\frac{1}{N} \sum_{n=1}^{N} Z_n^2} \quad (3)$$

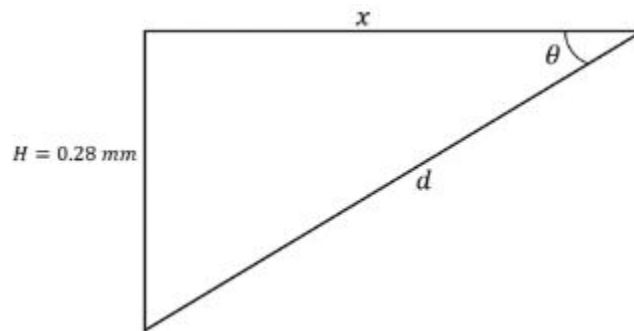Figure 19 is an image of one stair step to show the distance of one stair step per angle.

Figure 19: A graphical representation of a single stair step feature

Solve for the distance, d, to determine the distance of one stair step per angle.

$$sin\theta = \frac{0.28mm}{d} \quad (4)$$

$$d = \frac{0.28}{sin\theta}$$

θ is used in this project relates to the print angle, which consisted of 5°, 10°, 15°, 20°, 25°, and 30°. The distance for one stair step at the given angle are below:

5° has a one stair step distance of 3.2126 mm
10° has a one stair step distance of 1.6125 mm
15° has a one stair step distance of 1.0818 mm
20° has a one stair step distance of 0.8190 mm
25° has a one stair step distance of 0.6625 mm
30° has a one stair step distance of 0.5600 mm

Ra and Rq height were then calculated. The maximum allowed distance of the line profile given by the Keyence measuring tool is 0.5 inches or 12.7 mm. This is the distance that was used

to determine the number of stairs per given angle of length 12.7 mm.

We now show the calculation process for Ra and Rq for the 5° print angle. The other angles follow the same approach.

$$Number\ of\ Stairs = \frac{12.7\ mm}{3.2126} = 3.9683\ stairs \quad (5)$$
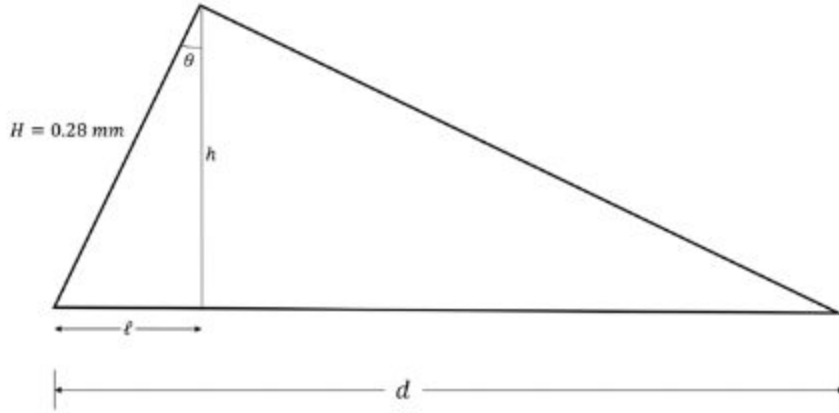

Figure 20: Determining distance of a stair step

The number of steps per angle in a 12.7 mm length are shown in Table 1.

Degree	Distance of Step (mm)	Number of Step
5°	3.213	3.95
10°	1.613	7.88
15°	1.082	11.74
20°	0.819	15.51
25°	0.663	19.17
30°	0.560	22.68

Table 1: Number of steps per given angle

Next, l and h are found to determine the equations of the piecewise function over the given reference length of 12.7 mm.

$$sin5° = \frac{l}{0.28\ mm} \quad \rightarrow \quad l = 0.0244 \quad (6)$$
$$cos5° = \frac{h}{0.28\ mm} \quad \rightarrow \quad h = 0.2789 \quad (7)$$

Equations of the piecewise function are below. There are eight equations used to make up the piecewise function. These eight equations are formulated by achieving the slope of each individual line and using the slope-intercept form to accomplish a line.

Equation of line 1a:

$$points : (0,0)\ and\ (0.0244,\ 0.2789)$$

110

$$slope\ (m) = \frac{0.2789-0}{0.0244-0} = 11.4317 \quad (8)$$

Slope intercept form:

$$y - y_1 = m(x - x_1) \quad (9)$$
$$y - 0.2789 = 11.4317(x - 0.0244) \quad (10)$$

Therefore, the equation of line 1a is:

$$y = 11.4307x \quad (11)$$

Equation of line 1b:

$$points : (0.0244,\ 0.2789)\ and\ (3.2126,\ 0)$$

The same procedure is used to obtain

$$y = -0.0875x + 0.2811 \quad (12)$$

The same method is carried out through all eight equations of the piecewise function and the remaining equations are as follows:

2a: $y = 11.4307x - 36.7211 \quad (13)$
2b: $y = -0.0875x + 0.5622 \quad (14)$
3a: $y = 114307x - 73.4420 \quad (15)$
3b: $y = -0.0875x + 0.8433 \quad (16)$
4a: $y = 11.4307x - 110.1629 \quad (17)$
4b: $y = -0.0875x + 1.1244 \quad (18)$

Twenty points were used to determine an accurate Ra and Rq value with increments of 0.635 mm. To calculate the Ra and Rq value, a Z_{mean} was calculated based on the $\frac{height\ (h)}{2}$. In this case, $Z_{mean} = 0.1395\ mm$. Thus Ra and Rq values are as follows for 5°:

$$Ra = 70.70$$
$$Rq = 81.19$$

The same procedure was carried out for all remaining angles (10°, 15°, 20°, 25°, and 30°) to achieve the Ra and Rq values, as seen in Table 2

	5°	10°	15°	20°	25°	30°
Ra	70.70	68.95	65.58	63.42	63.58	61.35
Rq	81.19	80.01	76.11	73.38	73.20	75.84

Table 2: Calculated values of Ra and Rq for idealized stair step features at given angles

From the literature, binder jetting parts can have green state densities between 44% and 57% [11]. We now consider an idealized model where the sand particles are taken as spheres. Since the packing factor of a simple cubic structure is 50%, we will model the packed sand as an array in a simple cubic structure. A rough direction can be posited as the direction diagonally across the unit cell as shown in Figure 21. The roughness calculation will be taken across the particles and gaps in this direction for a length of 12.7 mm. Figure 22 is a graphical visualization of the array of idealized sand particles along this orientation.
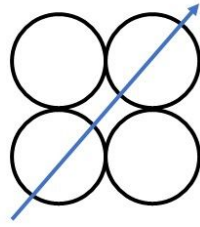
Figure 21: A left is a graphical representation of a simple cubic array of idealized sand particles. The arrow points in the direction that will be used in the calculations
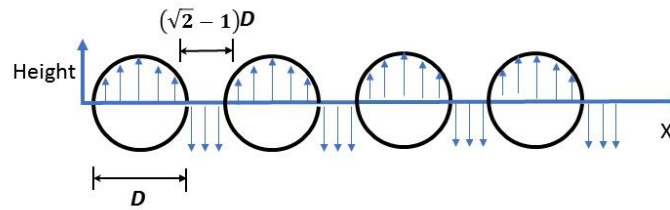

Figure 22: A depiction of idealized sand particles with gaps between them

Based on the the GFN of the sand used in the printing, the average particle diameter ranges from 150 μm to 170 μm. The same methodology is employed but with a piecewise height function of:

$$\text{For sand particles: } |Z| = \sqrt{\frac{D}{2}^2 + x^2} \quad (19)$$
$$\text{For gaps: } |Z| = \left|\frac{D}{2}\right| \quad (20)$$

where *D* is the idealized spherical sand particle diameter. The number of steps used was increased to *N*=40 because of the small size of the particles. The calculated values of Ra and Rq for 150 μm, 160 μm, and 170 μm are shown in Table 3.

	150 μm	**160** μm	**170** μm
Ra	61.61	67.60	71.22
Rq	64.28	70.04	74.06

Table 3: Calculated values of Ra and Rq for idealized close packed, spherical sand particles

The results from both the ideal stair step analysis and the ideal particle analysis are plotted as a function of print angle. Ra is shown in Figure 23. The average roughness of the idealized stair steps decreases as the angle increases. Ra for the idealized sand particles is not a function of print angle and is therefore constant. For all angles, Ra for the stair steps is less than those for idealized sand particles with a diameter of 170 μm. That diameter that is the high end of the particle size distribution. The Ra from the stair steps intersects that of the 160 μm idealized sand particles between 10 and 15°. The intersection for 150 μm is near 30°. This analysis appears

to correlate with the visual observation of stair steps disappearing into the background surface texture from the sand at angles greater than 15°.

Rq is shown in Figure 24. Rq from the stair steps does not reach the Rq values 150 μm or 160 μm at any angle. However, the stair step Rq does meet the value of Rq 170 μm around 20°. This may mean that Ra is more relevant to the visual appearance of the steps than Rq.

It should be noted that the calculated values of Ra and Rq for the idealized simple cubic sand particle array was much greater (2 to 2.5X) than the measured values for the most representative print angle: 0° (it would have no steps). This is not surprising in that real sand is not packed in a simple cubic array. Real sand is also not spherical in shape. The solidification of the casting and the resulting shrinkage would also be determining factors in smoothing the roughness of the casting.
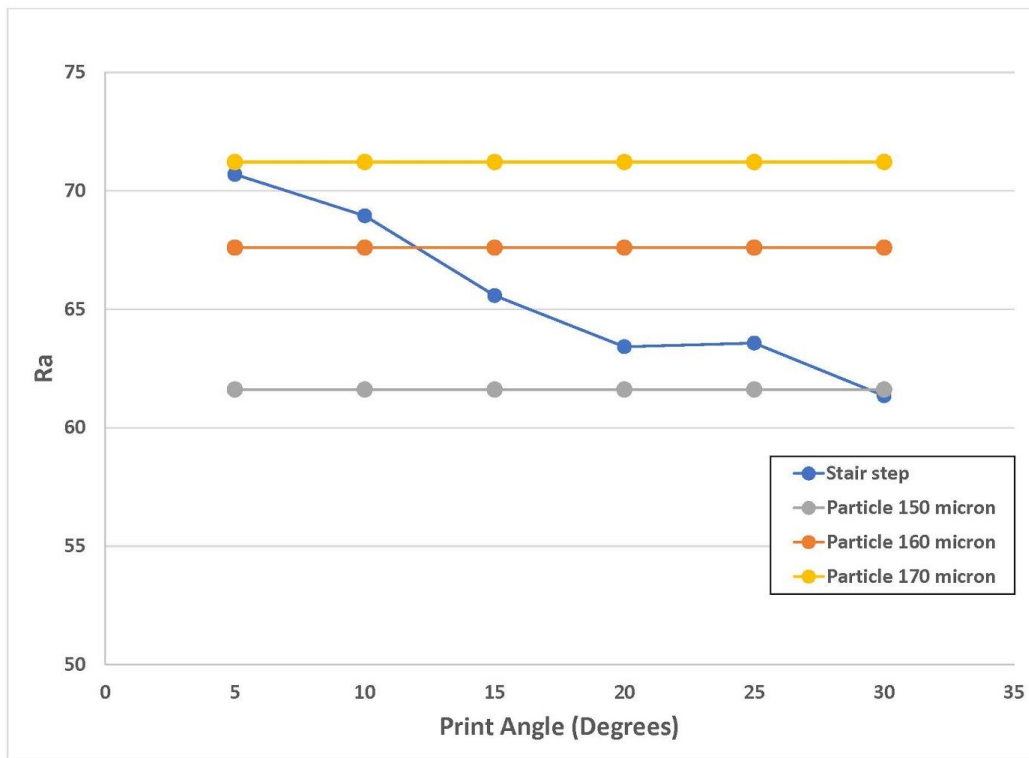

Figure 23: Calculated average roughness, Ra, plotted against print angle for the idealized stair step features and the idealized sand particles.
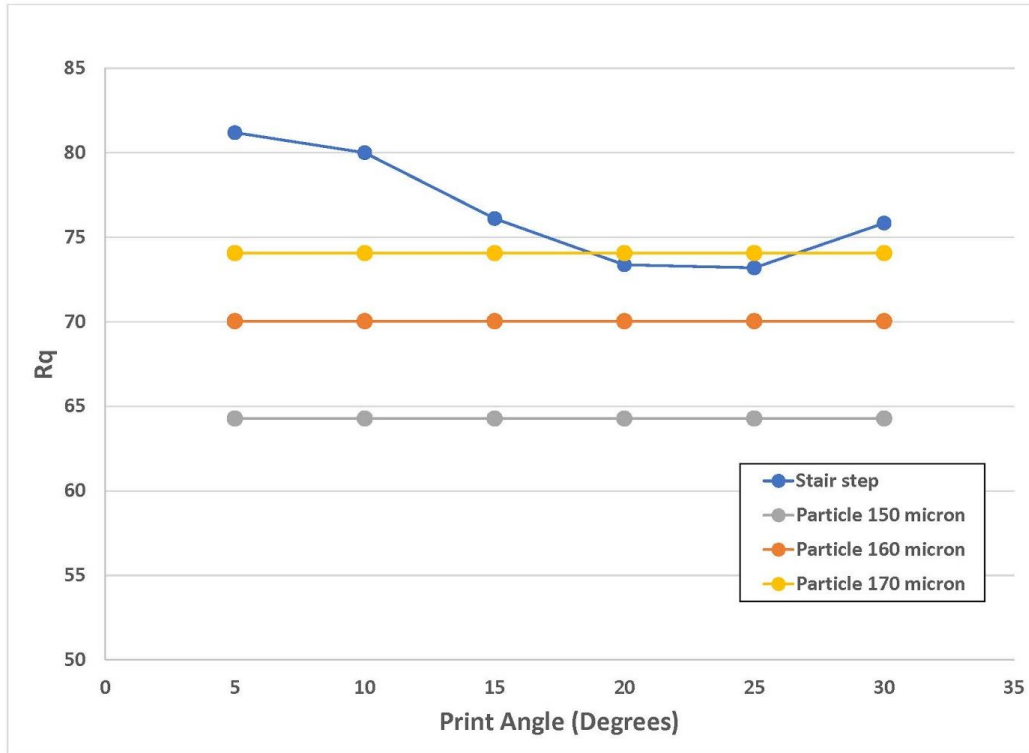
Figure 24: Calculated root mean squared roughness, Rq, plotted against print angle for the idealized stair step features and the idealized sand particles.

4. Conclusions

Several conclusions can be made from the observations above. First, stair step features are visually prominent on the cast surfaces at low values of print angle less than or equal to 15°. At higher angles they become visually indistinguishable from the background texture of the bound sand particles. Using the analytical calculations for Ra, it can be shown that at low print angles, the average roughness of a set of idealized stair step features will be greater than that for a idealized set of a simple cubic packed array of spherical sand particles with particle diameters of 150 μm or 160 μm.

It would be desirable to have a mathematical function for Ra and Rq that is dependent on the print angle (i.e. Ra(θ) and Rq (θ)). While it is possible to create a function dependent on print angle for Ra and Rq based on the idealized analysis, the variability in the measured surface roughness does not readily support such a function based on measurement.

For bare molds, upward facing surfaces on the castings had more visually prominent steps and higher Ra / Rq than downward facing surfaces. The possible reasons include: abrasive flow of molten metal onto upward mold steps facing downward casting surfaces, the cleaning

practices used to remove loose sand from molds, and the spreading of the furan binder from the stair step risers into the unbound sand causing a fillet in the mold (an observation noted in [8]).

The Dura Kote refractory coating did not erase the steps. The stair steps were still visible. This does not exclude the potential of other refractory coatings eliminating these steps. In most cases, the measured values of Ra and Rq for the castings with coated molds were generally less than those for bare molds.

Looking ahead, there are several areas still requiring research. First, there is a need to determine the effect of stair step features on static tensile and cyclic fatigue properties of a casting. It would be desirable to determine if a relationship exists between mechanical properties and the print angle. Second, more coatings need to be evaluated to determine if they can remove stair steps features thus eliminating subtractive post-processing operations specific to those features. Finally, it is also desirable to determine if the stair step features affect the performance of fluorescent penetrant inspection (FPI). In particular, it is important to answer two questions: 1.) Do the stair steps appear as linear indications? 2.) Does the background caused by the stair steps features hide actual linear indications?

DISCLAIMER

The views and conclusions contained in this document are those of the authors and should not be interpreted as necessarily representing the official policies, either expressed or implied, of the Government.

References

1. Census of world casting production: global casting production growth stalls. Modern Casting. Dec 2017: 24–28.

2. Banchhor R, Ganguly SK. Optimization in green sand casting process for efficient, economical and quality casting. Int J Adv Engg Tech/Vol V/Issue I/Jan -March. 2014;25:

29.

3. United States. Environmental Protection Agency. Office of Compliance. EPA Office of Compliance Sector Notebook Project: Profile of the metal casting industry. Office of Compliance, Office of Enforcement and Compliance Assurance, U.S. Environmental Protection Agency; 1997.

4. Almaghariz ES, Conner BP, Lenner L, Gullapalli R, Manogharan GP, Lamoncha B, et al. Quantifying the Role of Part Design Complexity in Using 3D Sand Printing for Molds and Cores. Int J Metalcast. 2016;10: 240–252.

5. Gullapalli RA. A Study of Mixed Manufacturing Methods in Sand Casting Using 3D Sand Printing and FDM Pattern-making Based on Cost and Time [Internet]. Youngstown State University. 2016. Available: http://rave.ohiolink.edu/etdc/view?acc_num=ysu1485335857475363

6. Walker J, Harris E, Lynagh C, Beck A, Lonardo R, Vuksanovich B, et al. 3D Printed Smart Molds for Sand Casting. Int J Metalcast. 2018; doi:10.1007/s40962-018-0211-x

7. ISO/ASTM. Standard Terminology for Additive Manufacturing – General Principles – Terminology. West Conshohocken, PA, 2015: ASTM International; 2015. Report No.: 52900-15.

8. Woods K. 3DPS Feature Generation in the YZ & XY Planes. Mod Cast. 2017;107: 36–40.

9. Jain PL. Principles of Foundry Technology. Tata McGraw-Hill Education; 2003.

10. Dura Kote 4482 Technical Data Sheet [Internet]. H A Interational LLC; 2018. Available: http://ha-international.com/tds/371234.pdf

11. Bai Y, Wagner G, Williams CB. Effect of Particle Size Distribution on Powder Packing and Sintering in Binder Jetting Additive Manufacturing of Metals. J Manuf Sci Eng. American Society of Mechanical Engineers; 2017;139: 081019.